New Journal of Physics
The open-access journal for physics

The CERN Super Proton Synchrotron as a tool to study high energy density physics

N A Tahir[1,7], R Schmidt[2], M Brugger[2], R Assmann[2], A V Shutov[3], I V Lomonosov[3], A R Piriz[4], D H H Hoffmann[5], C Deutsch[6] and V E Fortov[3]

[1] Gesellschaft für Schwerionenforschung, Planckstrasse 1, 64291 Darmstadt, Germany
[2] CERN–AB, 1211 Geneva, Switzerland
[3] Institute of Problems of Chemical Physics, Chernogolovka, Russia
[4] ETSI Industriales, Universidad de Castilla-La Mancha, 1307 Ciudad Real, Spain
[5] Institut für Kernphysik, TU Darmstadt, 64289 Darmstadt, Germany
[6] Laboratoire de Physique des Gaz et des Plasmas, Universite Paris–Sud, 91405 Orsay, France
E-mail: n.tahir@gsi.de

New Journal of Physics **10** (2008) 073028 (11pp)
Received 5 May 2008
Published 15 July 2008
Online at http://www.njp.org/
doi:10.1088/1367-2630/10/7/073028

Abstract. An experimental facility named HiRadMat, will be constructed at CERN to study the impact of the 450 GeV c^{-1} proton beam generated by the Super Proton Synchrotron (SPS) on solid targets. This is designed to study damage caused to the equipment including absorbers, collimators and others in case of an accidental release of the beam energy. This paper presents two-dimensional numerical simulations of target behavior irradiated by the SPS beam. These numerical simulations have shown that the target will be completely destroyed in such an accident, thereby generating high energy density (HED) matter. This study therefore suggests that this facility may also be used for carrying out dedicated experiments to study HED states in matter.

[7] Author to whom any correspondence should be addressed.

Contents

1. Introduction

The Super Proton Synchrotron (SPS) at CERN is used as injector to the Large Hadron Collider (LHC) as well as accelerating protons for neutrino production (CNGS project). For LHC injection, the proton bunches are accelerated to a momentum of 450 GeV c^{-1} and are transferred to the LHC via two beam lines. Several SPS cycles will be required to fill the LHC while in one cycle, a batch of 288 bunches can be accelerated. Such batches are extracted from the SPS by a fast kicker magnet and transferred via a 3 km long beam line into the LHC injection point. A second fast kicker magnet deflects the beam into the LHC. Although the energy stored in the batch is less than 1% of the LHC beam energy at 7 TeV c^{-1}, it is still sufficient to cause considerable damage in case of a failure. To assess the damage level caused by such an accident, limited experiments on target irradiation by the SPS beam have been done in a beam transfer line between the SPS and the LHC/CNGS target [1, 2]. This will not be possible in years to come, whereas such studies will be required on regular basis. For this reason, a facility for tests with extreme thermomechanical shocks, named HiRadMat, is being constructed as part of the phased implementation for LHC collimators [3]. It will allow a several mega joules energy beam to be sent in microsecond pulses to a dedicated target station that will be constructed. The main use of this facility will be to test the consequences of beam impact on beam absorbers, collimators and other objects, which is mandatory for the design of such devices to be installed in the LHC and other future accelerator facilities like FAIR, at Darmstadt [4]. These experiments therefore will be very useful for validating simulations that have been previously done to estimate damage caused by an LHC beam in case of an accident [5, 6]. In addition to that, other areas of research including material sciences and high energy density (HED) states in matter will also benefit from these experiments. In this paper, we present numerical simulations of hydrodynamic and thermodynamic responses of a solid tungsten target that has been irradiated with full SPS beam. These simulations have shown that the target will be completely destroyed generating large samples of HED matter.

In section 2, we present the SPS beam parameters and the problem of energy loss by highly relativistic protons in solid tungsten is discussed in section 3. Numerical simulation results of thermodynamic and hydrodynamic responses of a solid tungsten target are presented in section 4 while conclusions drawn from this work are noted in section 5.

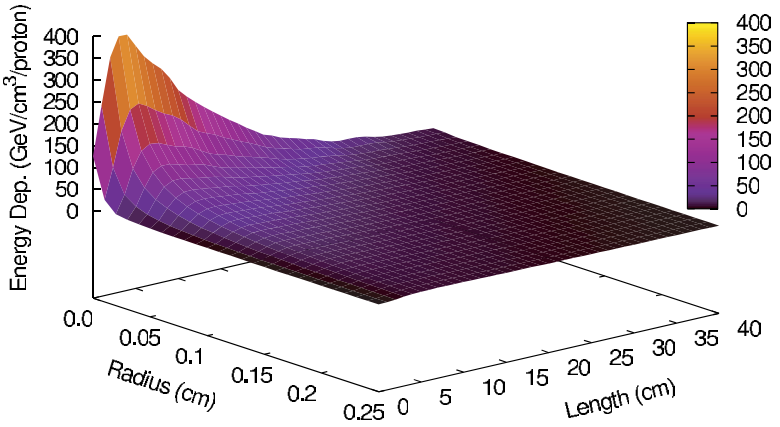

Figure 1. Energy deposition by a single 450 GeV c^{-1} proton (GeV $proton^{-1}$ cm^{-3}) in solid tungsten as calculated by the FLUKA code [7, 8]; beam focal spot (σ) = 0.088 mm.

2. The SPS at CERN

The SPS is used as LHC injector, but also to accelerate and extract protons and ions for fixed target experiments and for producing neutrinos (CNGS). In particular, the risks during the fast extraction of LHC and CNGS beams must be considered since any failure during this process can lead to serious equipment damage.

The SPS accelerator is 6.9 km long (circumference) and accelerates protons from 14 or 26 GeV c^{-1} to a momentum of up to 450 GeV c^{-1}. It is a cycling machine with cycles having a length of about 10 s. The transverse beam size is largest at injection and decreases with the square root of the beam energy during acceleration. For operation as a synchrotron, the beam size is typically of the order of 1 mm.

When the SPS operates as LHC injector, up to 288 bunches are accelerated, each bunch with about 1.1×10^{11} protons. The bunch length is 0.5 ns and two neighboring bunches are separated by 25 ns so that the duration of the entire beam is about 7 μs. The normalized emittance is 3.75×10^{-6} m. Assuming a beta function of 100 m, the beam size (σ of the Gaussian intensity distribution) is 0.88 mm. When the SPS was used as a proton–antiproton collider, the luminosity was maximized by minimizing the beta function to 0.5 m. Assuming this value the beam size would be about 0.06 mm. In the work presented in this paper, we consider two cases, namely, σ = 0.088 and 0.88 mm, respectively.

3. Energy deposition by protons in tungsten

High-energy protons impinging on the studied material samples produce particle cascades depositing their energy in matter that leads to an increase in temperature. The required energy deposited by the 450 GeV c^{-1} SPS beam as a function of material and geometry has been calculated using the FLUKA code [7, 8]. This is a fully integrated particle physics and multi-purpose Monte Carlo simulation package capable of simulating all components of the particle cascades in matter up to TeV energies. Further details can be found elsewhere [7, 8].

Figure 1 shows the energy deposition by a single 450 GeV c^{-1} proton (in a beam with σ = 0.088 mm) and the shower it creates in a solid tungsten cylindrical target that is 50 cm

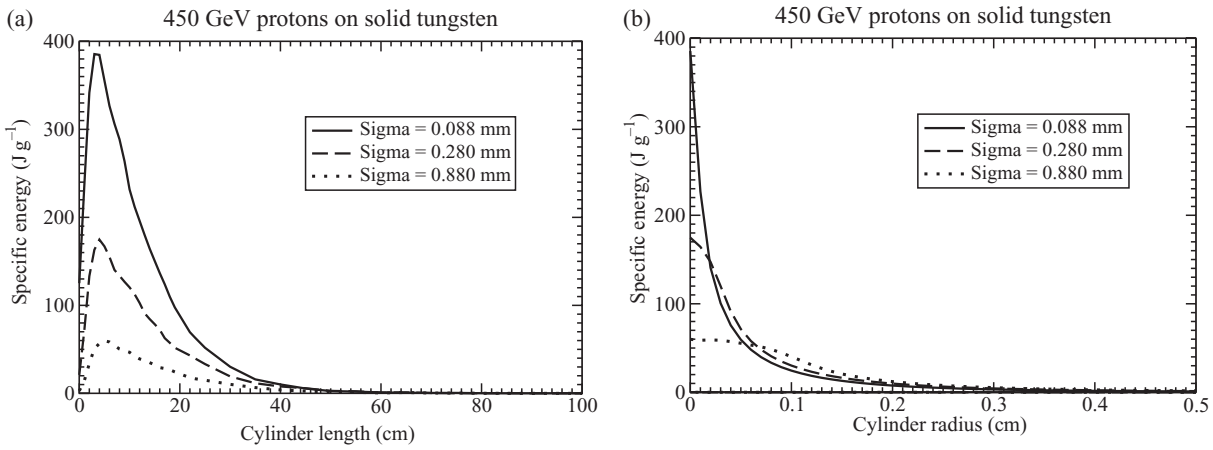

Figure 2. Specific energy deposition by a single bunch considering three different values of beam focal spot: (a) along beam axis at $r = 0.0$; (b) along radius at $L = 5$ cm (the point of maximum deposition).

long and has a radius = 5 mm. Figure 2 shows the specific energy deposition by a single bunch that consists of 1.1×10^{11} protons assuming three different values of σ of the Gaussian transverse intensity distribution, namely, 0.088 mm, 0.28 mm and 0.88 mm, respectively. The focal spot sizes corresponding to these values are within the typical operational limits of the SPS proton–antiproton collider. To obtain the smallest beam sizes in HiRadMat, additional quadrupole magnets need to be installed. The bunch length is 0.5 ns while two neighboring bunches are separated by 25 ns so that the total pulse length is about 7 μs.

4. Numerical simulation results of thermodynamic and hydrodynamic responses of solid tungsten target

In this section, we present numerical simulation results of thermodynamic and hydrodynamic behavior of a solid tungsten cylindrical target with a radius = 5 cm and a length = 50 cm that is facially irradiated by the SPS proton beam. These simulations have been carried out using a two-dimensional hydrodynamic computer code, BIG-2 [9]. Two different beam focal spot sizes corresponding to σ of the transverse particle intensity distribution equal to 0.088 and 0.88 mm respectively, have been considered. The results are presented below.

4.1. Using focal spot 0.088 mm

Protons lose energy in the target as well generating a shower of secondary particles which are eventually absorbed by the target material. The specific energy deposited by a single bunch along the beam axis (at $r = 0.0$) and along the radial direction (at the point of maximum energy deposition in the L direction), are shown in figures 2(a) and (b), respectively. It is seen that a specific energy of 0.38 kJ g^{-1} is deposited at the beam axis at $L = 10$ cm, where the maximum energy deposition occurs. Energy deposition in the material leads to a substantial increase in the target temperature.

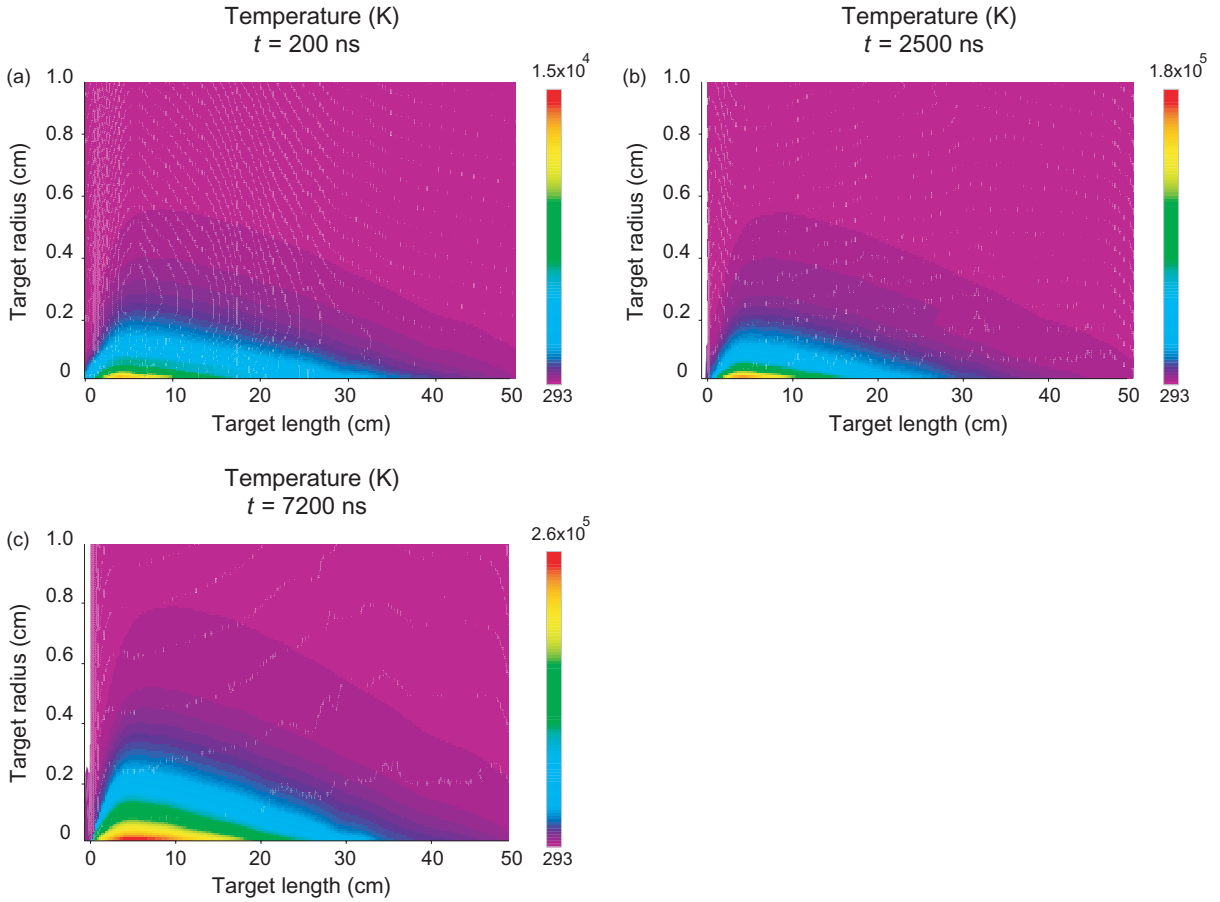

Figure 3. Beam incident from left-to-right: temperature on length–radius plane, solid tungsten cylindrical target facially irradiated by 450 GeV c^{-1} SPS proton bunches, target length = 50 cm, target radius = 5 cm, Gaussian intensity distribution in transverse direction with $\sigma = 0.088$ mm, 288 bunches with each bunch composed of 1.1×10^{11} protons, bunch length = 0.5 ns, bunch separation = 25 ns; (a) $t = 200$ ns; (b) $t = 2500$ ns and (c) $t = 7.2$ μs which is the end of the pulse; (any significant temperature variation is localized to the beam-heated region so only the inner 1 cm radius is shown in these figures).

In figure 3, we plot the target temperature on a length–radius plane at three different times during beam irradiation. Figure 3(a) is plotted at $t = 200$ ns, a time when 8 out of 288 bunches have been delivered. It is seen that the maximum temperature of about 1.5×10^4 K is generated in the beam heated region. Figure 3(b) shows that the temperature increases to 1.8×10^5 K at $t = 2500$ ns when 100 bunches have been delivered whereas figure 3(c) shows that at the end of the SPS beam at $t = 7200$ ns, the maximum temperature increases to a value of 2.6×10^5 K.

Temperature profiles along the beam axis ($r = 0.0$) at various times during irradiation are presented in figure 4(a) whereas temperature variations in the radial direction at $L = 5$ cm are shown in figure 4(b). Simulations show that the SPS beam with this focal spot deposits about 100 kJ g^{-1} specific energy in the target which is comparable with that deposited by the uranium beam at a dedicated facilities like SIS18 [10]–[12] and FAIR [13]–[16] at Darmstadt.

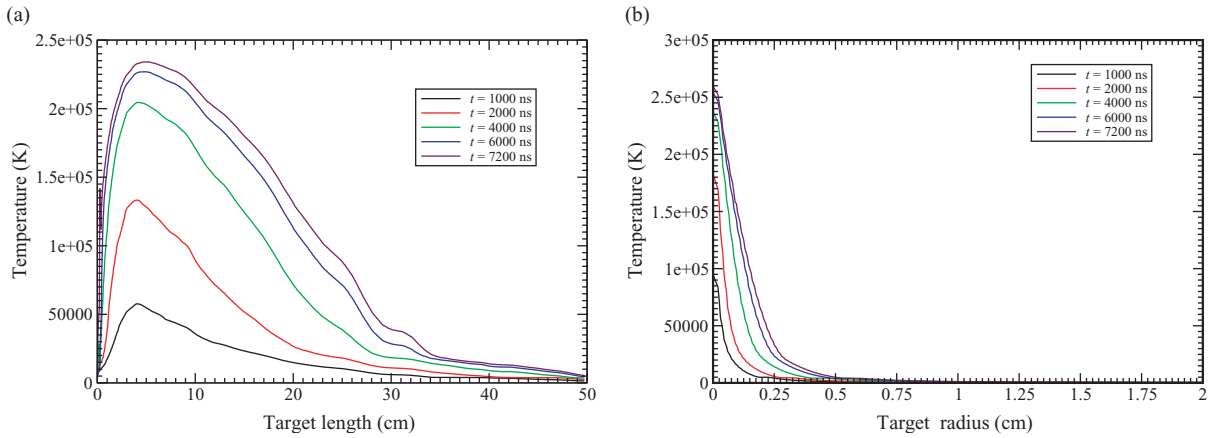

Figure 4. Temperature profiles at different times corresponding to figure 3, (a) along axis ($r = 0.0$) and (b) along radius ($L = 5$ cm).

The high temperature in the beam heated region generates very high pressure that launches a strong radial shock wave. Pressure corresponding to the target temperature presented in figure 3 is plotted in figure 5. It is seen in figure 5(a) that a maximum pressure of 32 GPa is generated at the beam axis at $t = 200$ ns. Figure 5(b) shows that the shock wave has moved outwards to a position, $r = 1$ mm while the maximum pressure has been reduced to a value of 12 GPa, due to cylindrical divergence. It is seen from figure 5(c) that by the end of the SPS beam (at $t = 7200$ ns), the shock wave has moved out to a radial position $r = 3$ mm, whereas the maximum pressure is now 7 GPa. We note that target heating is a localized effect as electron heat conduction is not so effective on this timescale. We therefore only show the inner 1 cm radius of the target for temperature profiles. Pressure propagation, on the other hand, is not localized to the beam interaction region and therefore we show the target behavior within the full radius of 5 cm. To evaluate quantitative variation of the pressure along the longitudinal and radial directions we plot respective profiles in figures 6(a) and (b), respectively, at different times during the target irradiation.

Target density on a length–radius plane at two different times is shown in figures 7(a) and (b), respectively. It is seen in figure 7(a) that at $t = 2500$ ns, when 100 out of 288 bunches have been delivered, the target density along the target axis has been reduced to less than 10% of the solid density. This is because the shock wave moves the material away from the target center which means that the subsequent proton bunches will penetrate longer distances into the target. This range lengthening due to hydrodynamic motion will have very important implications on design of collimators and sacrificial beam stoppers and must be considered in such designs. Figure 7(b) shows that the target density decreases to about 1% of the solid density at the end of the SPS pulse. In order to estimate the density variation in the longitudinal and radial directions in a more quantitative manner, corresponding profiles at different times are presented in figures 8(a) and (b), respectively.

In figure 9, we show the target physical state at the end of the proton pulse at $t = 7200$ ns. It is seen that within the inner 2 mm radius, a strongly coupled plasma state exists that is followed by an expanded hot liquid. The melting front is also seen propagating outwards. The physical states have been calculated using a sophisticated semi-empirical equation-of-state (EOS) model described elsewhere [17]. These simulations clearly show that an SPS proton beam is capable

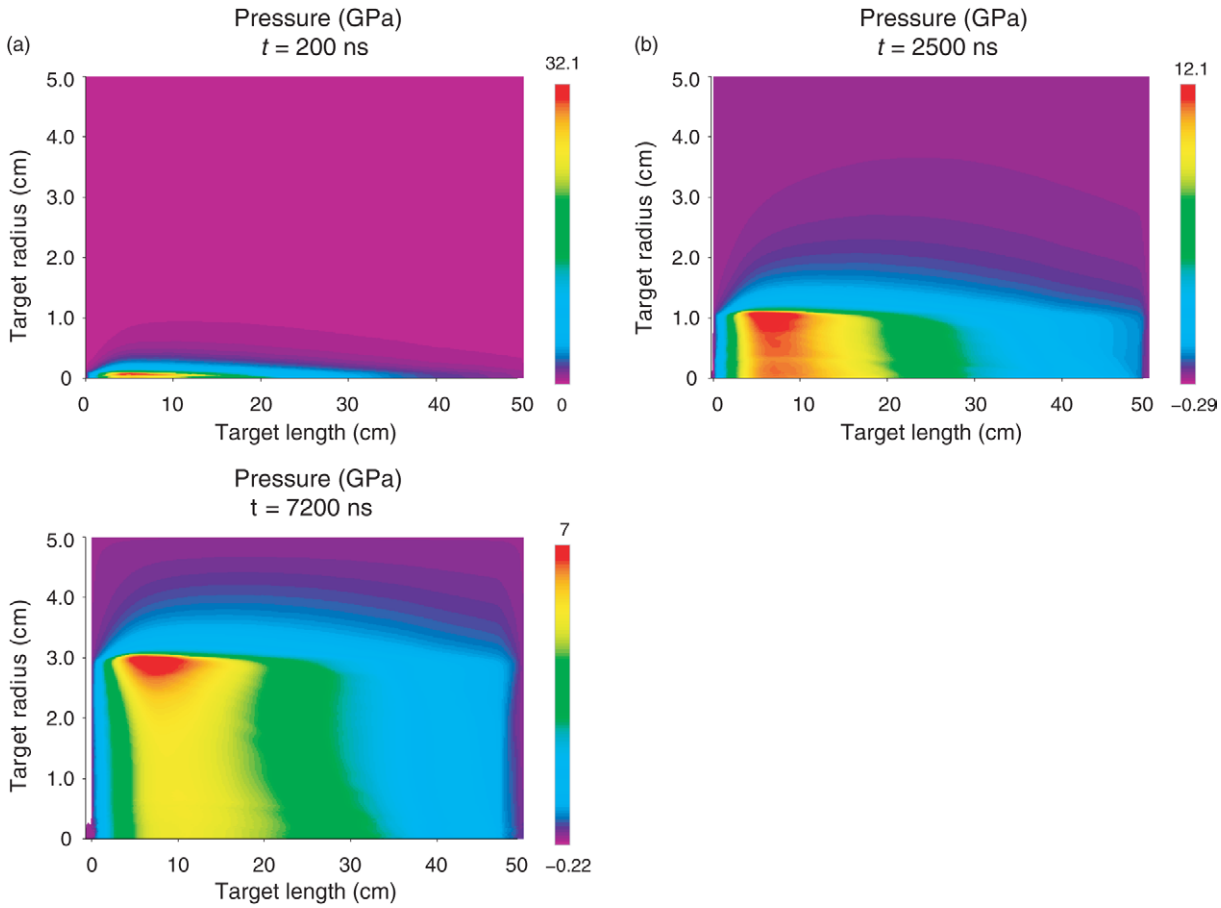

Figure 5. Beam incident from left-to-right: pressure on length–radius plane, solid tungsten cylindrical target facially irradiated by 450 GeV c^{-1} SPS proton bunches, target length = 50 cm, target radius = 5 cm, Gaussian intensity distribution in transverse direction with $\sigma = 0.088$ mm, 288 bunches with each bunch composed of 1.1×10^{11} protons, bunch length = 0.5 ns, bunch separation = 25 ns; (a) $t = 200$ ns; (b) $t = 2500$ ns and (c) $t = 7.2\,\mu$s which is the end of the pulse. (Propagation of shock wave generated by thermal pressure is clearly seen.)

of destroying solid targets, leading to generation of interesting HED states in matter. It will therefore be possible to perform dedicated HED experiments at the future HiRadMat facility at CERN.

4.2. Using focal spot 0.88 mm

Simulations have also been carried out using a larger focal spot corresponding to $\sigma = 0.88$ mm. The temperature profiles in the longitudinal and radial directions at different times are presented in figures 10(a) and (b), respectively. It is seen that at the end of the pulse, a maximum temperature of about 10^5 K is generated at the target axis that is sufficient to generate HED matter.

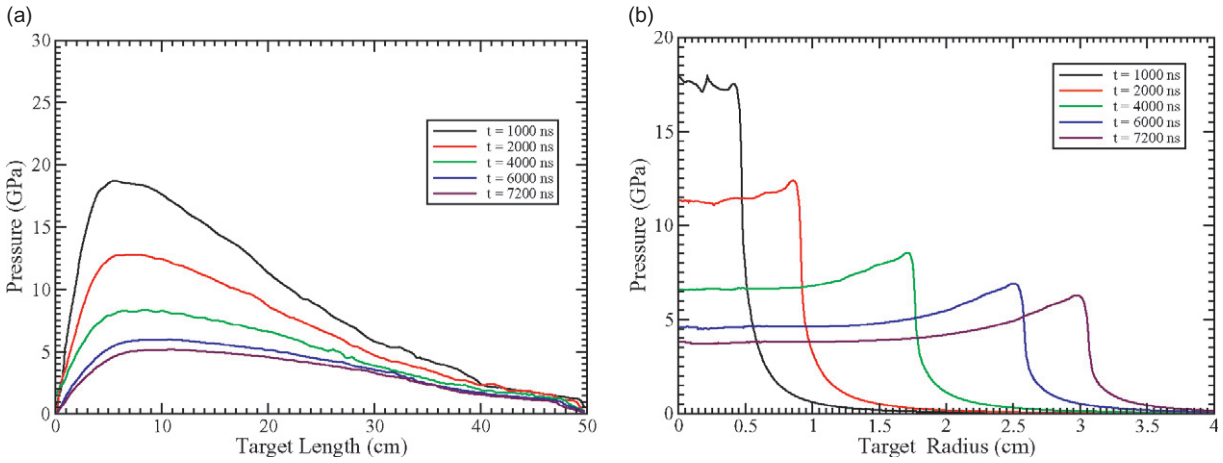

Figure 6. Pressure profiles at different times corresponding to figure 5, (a) along axis ($r = 0.0$) and (b) along radius ($L = 5$ cm).

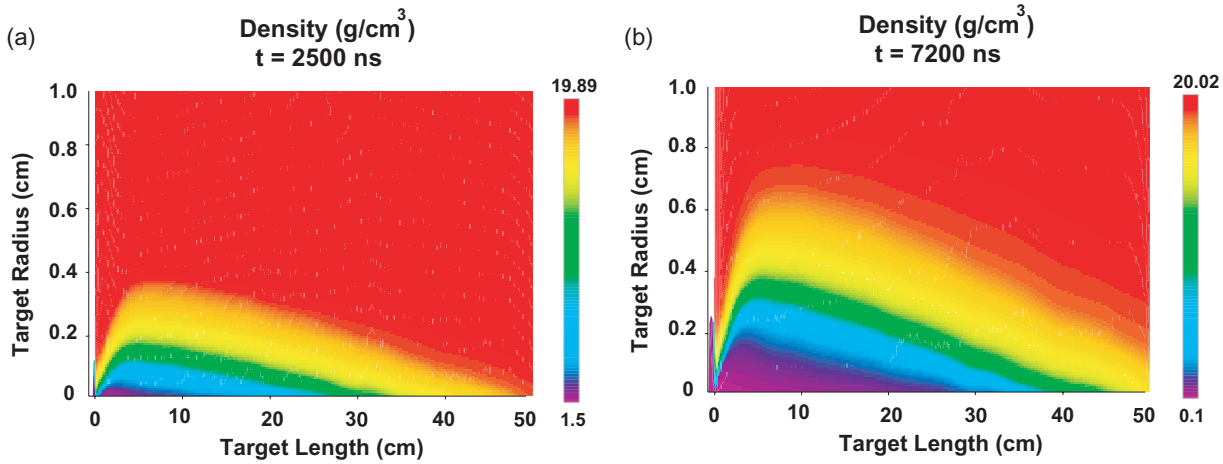

Figure 7. Beam incident from left-to-right: density on length–radius plane corresponding to figure 4; (a) $t = 2500$ ns and (b) $t = 7.2\,\mu$s which is the end of the pulse (any significant density variation is localized to beam-heated region so only the inner 1 cm radius is shown in these figures).

The corresponding pressure profiles are plotted in figures 11(a) and (b), respectively. It is seen that a maximum pressure of about 25 GPa is generated at $t = 400$ ns that launches a strong shock wave in the radial direction. It is to be noted that the maximum pressure in the case of $\sigma = 0.088$ mm is achieved at $t = 200$ ns. Radially outward propagation of the shock wave is seen in figure 11(b).

The density profiles are plotted in figures 12(a) and (b), respectively that show that even in this case, the density at the target center is substantially reduced due to the radial shock wave. However, the minimum density now is about 10% of the solid tungsten density.

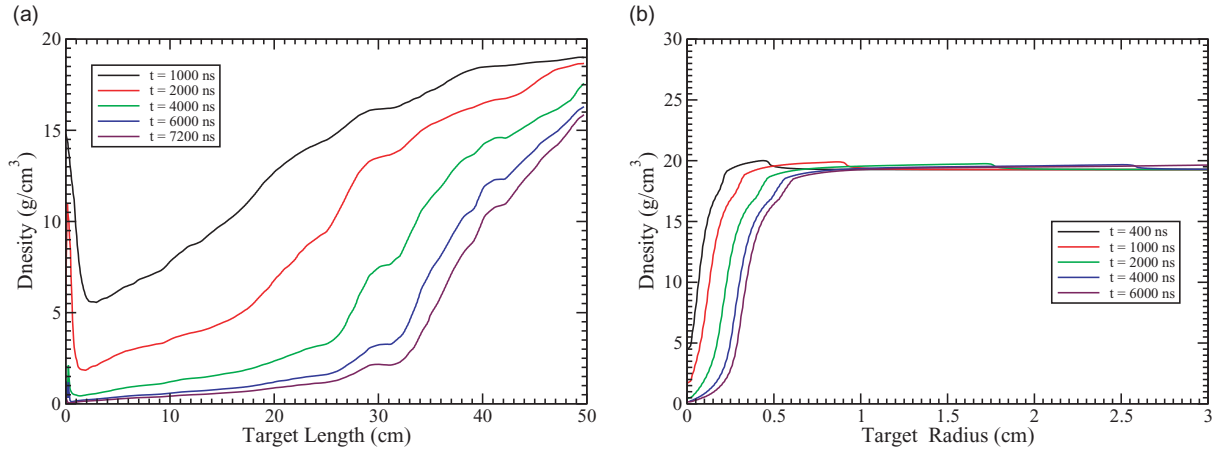

Figure 8. Density profiles at different times corresponding to figure 7, (a) along axis ($r = 0.0$) and (b) along radius ($L = 5$ cm).

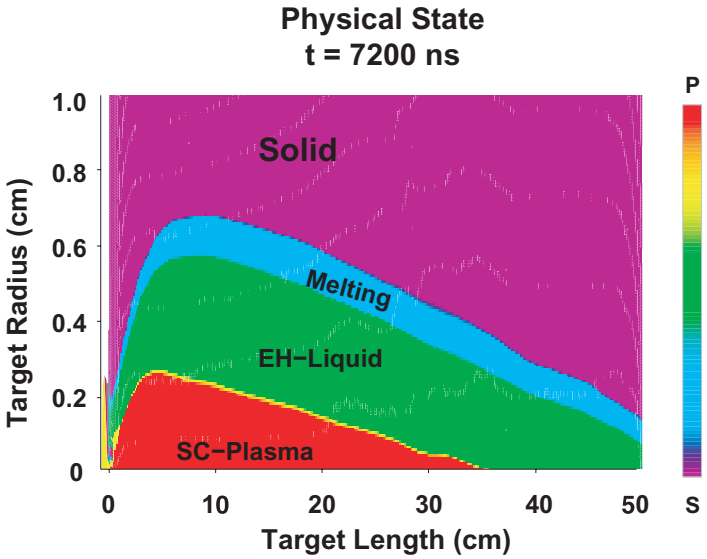

Figure 9. Target physical state at $t = 7.2\,\mu$s with $\sigma = 0.088$ mm.

4.3. Further discussion of results

In these simulations, the proton energy loss has been calculated using the FLUKA code assuming fixed solid target density. These data are used as input to the hydrodynamic code, BIG2, to simulate the target behavior. The simulations, however, have shown that the target density changes significantly due to onset of hydrodynamic motion during target irradiation. More precise calculations that use FLUKA and BIG2 codes interactively are therefore necessary. This work is in progress.

It is to be noted that an SPS beam could be very useful to supplement heavy ion beams at FAIR to study EOS properties using a HIHEX-type scheme [14]–[16]. In this proposed scheme, the HED states are generated by heating and expansion of the target material. However, unlike heavy ions, protons are not very suitable for performing compression experiments, for example, those proposed in a LPLAS scheme [18]–[23] at FAIR.

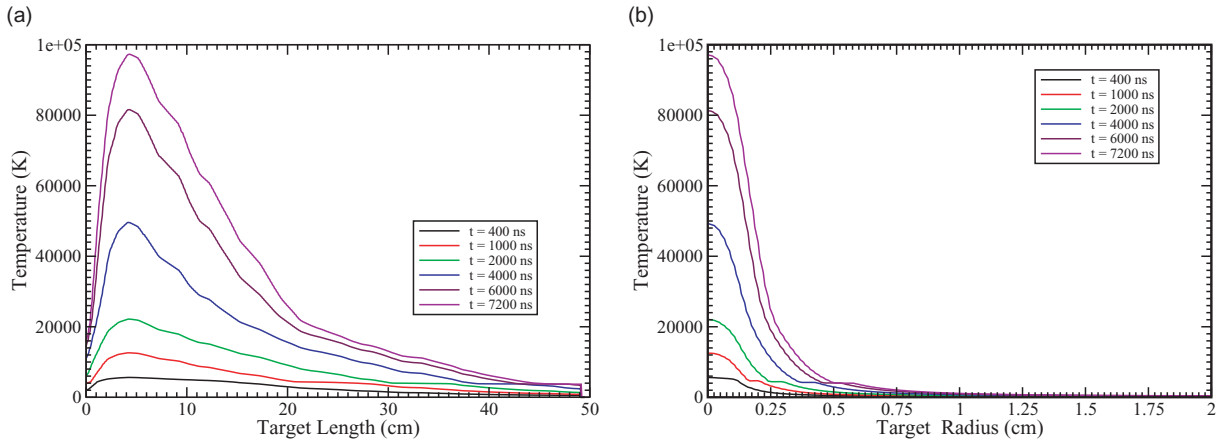

Figure 10. Temperature profiles at different times using $\sigma = 0.88$ mm, (a) along axis ($r = 0.0$) and (b) along radius ($L = 5$ cm).

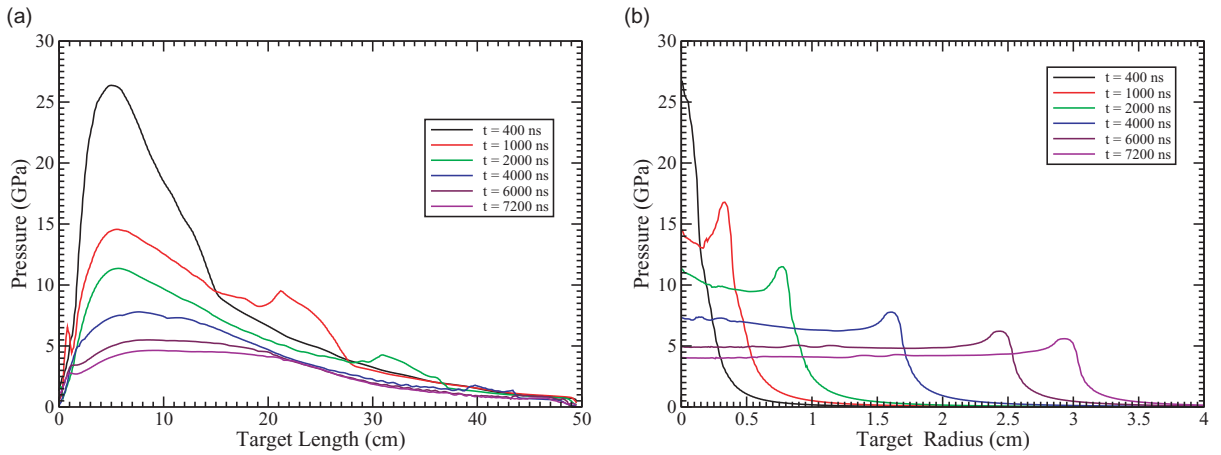

Figure 11. Pressure profiles at different times using $\sigma = 0.88$ mm, (a) along axis ($r = 0.0$) and (b) along radius ($L = 5$ cm).

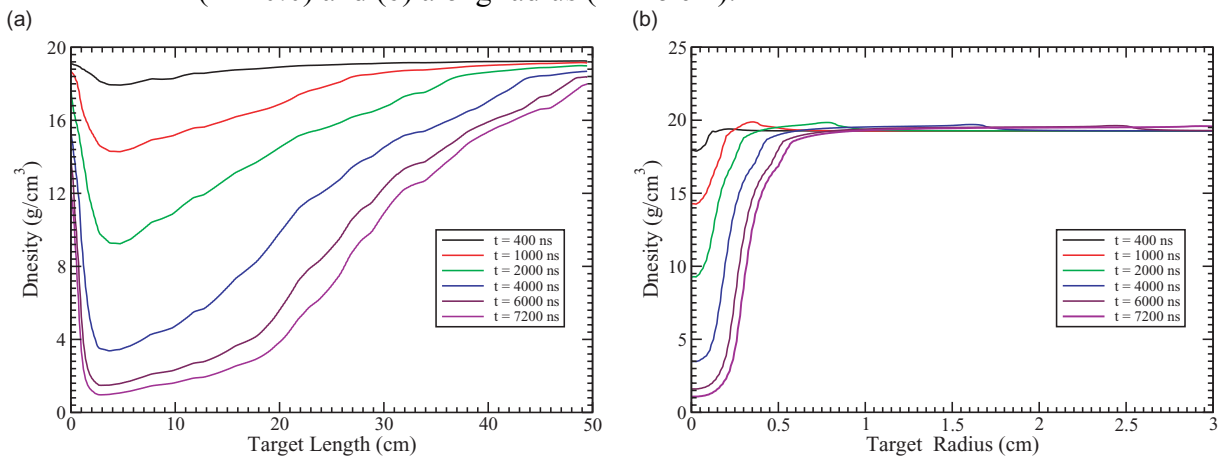

Figure 12. Density profiles at different times using $\sigma = 0.88$ mm, (a) along axis ($r = 0.0$) and (b) along radius ($L = 5$ cm).

5. Conclusions

Simulations presented in this paper have shown that the proton beam generated by the SPS has the potential to completely destroy solid targets. It has been shown that the high pressure generated in the target due to energy deposition by the first few bunches will drive an outward radial shock wave that will lead to a substantial reduction in density at the target center. The protons delivered in subsequent bunches will therefore penetrate longer distance in the material. This phenomenon should be considered while designing collimators and sacrificial beam stoppers.

Another important outcome of this work is that the SPS beam can generate HED matter and dedicated experiments can be carried out at the HiRadMat facility to study this important subject.

References

[1] Kain V *et al* 2005 *CERN-LHC-Project-Report 822* (Geneva: CERN)
[2] Assmann R *et al* 2005 LHC Collimators: design and results from prototyping and beam tests, *CERN-LHC-Project Report-850* (Geneva: CERN)
[3] Assmann R 2007 Private communication
[4] Henning W F 2004 *Nucl. Instrum. Methods* A **214** 211
[5] Tahir N A *et al* 2005 *J. Appl. Phys.* **97** 083532
[6] Tahir N A *et al* 2005 *Phys. Rev. Lett.* **94** 135004
[7] Fasso A *et al* 2005 FLUKA: a multi-particle transport code *CERN-2005-10*, INFN/TC-05/11, SLAC-R-773
[8] Fasso A *et al* 2003 The physics models of FLUKA: status and recent developments *Conf. on Computing in High Energy and Nuclear Physics, La Jolla, USA, 24–28 March* (*Preprint* hep-ph/0306267)
[9] Fortov V E *et al* 1996 *Nucl. Sci. Eng.* **123** 169
[10] Tahir N A *et al* 1999 *Phys. Rev.* E **60** 4715
[11] Tahir N A *et al* 2000 *Phys. Rev.* E **61** 1975
[12] Tahir N A *et al* 2000 *Phys. Rev.* E **62** 1224
[13] Tahir N A *et al* 2003 *Phys. Rev. ST Accel. Beams* **6** 020101
[14] Tahir N A *et al* 2005 *Phys. Rev. Lett.* **95** 035001
[15] Tahir N A *et al* 2005 *Nucl. Instrum. Methods* A **544** 16
[16] Tahir N A *et al* 2007 *Nucl. Instrum. Methods* A **577** 238
[17] Lomonosov I V 2007 *Laser Part. Beams* **25** 567
[18] Tahir N A *et al* 2001 *Phys. Rev.* E **63** 036407
[19] Tahir N A *et al* 2003 *Nucl. Instrum. Methods* B **204** 282
[20] Piriz A R *et al* 2002 *Phys. Rev.* E **66** 056403
[21] Piriz A R *et al* 2002 *Laser Part. Beams* **20** 427
[22] Piriz A R *et al* 2003 *Plasma Phys. Control. Fusion* **45** 1733
[23] Piriz A R *et al* 2003 *Phys. Rev.* E **67** 017501